JOURNAL OF MORPHOLOGY 267:649–662 (2006)

Spatial and Functional Modeling of Carnivore and Insectivore Molariform Teeth

Alistair R. Evans* and Gordon D. Sanson

School of Biological Sciences, Monash University, Clayton Campus, Victoria 3800, Australia

ABSTRACT The interaction between the two main competing geometric determinants of teeth (the geometry of function and the geometry of occlusion) were investigated through the construction of three-dimensional spatial models of several mammalian tooth forms (carnassial, insectivore premolar, zalambdodont, dilambdodont, and tribosphenic). These models aim to emulate the shape and function of mammalian teeth. The geometric principles of occlusion relating to single- and double-crested teeth are reviewed. Function was considered using engineering principles that relate tooth shape to function. Substantial similarity between the models and mammalian teeth were achieved. Differences between the two indicate the influence of tooth strength, geometric relations between upper and lower teeth (including the presence of the protocone), and wear on tooth morphology. The concept of "autocclusion" is expanded to include any morphological features that ensure proper alignment of cusps on the same tooth and other teeth in the tooth row. It is concluded that the tooth forms examined are auto-aligning, and do not require additional morphological guides for correct alignment. The model of therian molars constructed by Crompton and Sita-Lumsden ([1970] Nature 227:197–199) is reconstructed in 3D space to show that their hypothesis of crest geometry is erroneous, and that their model is a special case of a more general class of models. J. Morphol. 267:649–662, 2006. © 2004 Wiley-Liss, Inc.

KEY WORDS: modeling; functional morphology; dental; dentition; autocclusion; mammal; VRML; 3D

Teeth are attractive as study subjects for many and varied reasons, including their substantial contribution to the vertebrate fossil record and their intriguing developmental processes (Butler, 1981; Fortelius, 1985; Jernvall, 1995). Another notable reason is the four-dimensional puzzles they present. Teeth have complex three-dimensional geometries that interlock with their occluding counterparts in a temporal sequence. Perhaps more important, the purpose of the geometry of the dentition is to perform several functions, the most significant of which is the efficient break-down of food (Lucas, 1979).

Various aspects of tooth geometry and occlusion have been investigated for tooth forms, including tribosphenic-like (Crompton and Sita-Lumsden, 1970; Kay and Hiiemae, 1974; Crompton et al., 1994), herbivore (Greaves, 1972; Fortelius, 1985), and carnivore molariform teeth (Mellett, 1981, 1985; Bryant and Russell, 1995). Certain geometric principles were established in these articles, but several of the predictions made appear to have remained untested. Also, there does not seem to be a clear understanding of all geometric aspects of occlusion in many tooth forms. No comprehensive analysis of these principles has been carried out, nor any investigation of their implications. For example, we would like to know what dental shapes are feasible given certain geometric constraints; i.e., what are the limits to possible occlusal morphologies?

The tooth form of occluding "primitive" therian teeth has been considered as a set of "reversed triangles" (Fig. 1a; Crompton and Sita-Lumsden, 1970; Crompton et al., 1994). This notion formed part of the "trituberculy" theory of dental evolution (Osborn, 1888, 1897; Gregory, 1916), in which it was hypothesized that the ancestral dental shape of therians was of this form. However, many features of the geometry of occlusion and the full ramifications of the "reversed triangle" design appear not to have been evaluated. The study of Crompton and Sita-Lumsden (1970) modeled the two-bladed basic therian molar pattern as reversed triangles (each cusp is basically triangular and has two blades, the diagonal and transverse shearing edges, leading down from it; Fig. 1b). It was concluded that it would be impossible for both of the blades on such a molar to be two-dimensional curves: a 2D curve is one that lies within a plane and is curved in only two dimensions rather than three, such as the letter "S" and a scimitar blade. If so, this would greatly limit the possible tooth and crest shapes, but the hypothesis has not been tested.

In order to deal with the complexity and diversity of mammalian tooth forms, it is necessary to eluci-

Supplementary material for this article is available from the first author or via the Internet at http://www.interscience.wiley.com/jpages/0362-2525/suppmat

*Correspondence to: Dr. Alistair Evans, Institute of Biotechnology, University of Helsinki, P.O. Box 56 (Viikinkaari 9), FIN-00014 University of Helsinki, Helsinki, Finland. E-mail: arevans@fastmail.fm

Published online 29 November 2004 in
Wiley InterScience (www.interscience.wiley.com)
DOI: 10.1002/jmor.10285

© 2004 WILEY-LISS, INC.

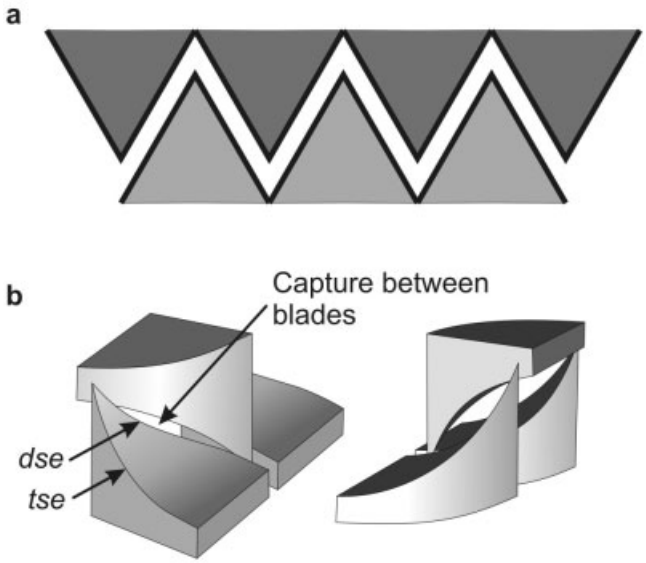

Fig. 1. **a:** The "reversed triangles" model of molar occlusion, with upper (dark) and lower (light) molars in a triangular shape and the thick lines representing blades. **b:** The Crompton and Sita-Lumsden (1970) model of therian molar function. dse, diagonal shearing edge; tse, transverse shearing edge. Redrawn from Crompton and Sita-Lumsden (1970).

date some basic geometric principles of teeth. We suggest that there are two main competing geometric factors that influence dental morphology: the geometry of occlusion (ensuring proper alignment of tooth features such as crests) and the geometry of function (relating to shape that is advantageous for food fracture, thereby minimizing force or energy for a tooth to fracture food). These can be considered separately by examining the features that influence occlusal geometry and those that relate to function. However, the ultimate goal is to understand how these interact in order to limit the forms that can be expressed, a minimum set of which actually occurs in animals.

This article first explains the basic geometric principles of teeth, which have been expounded to some extent in the literature. We will investigate the important geometrical relations between occluding tooth components through the generation of hypotheses in the form of geometric models of teeth that consider the form and manner of tooth function. Using these geometric principles, as well as aspects of shape that affect function, models of several tooth forms will be constructed, principally carnivore and insectivore molars and premolars. Mathematical geometry (e.g., planes and vectors) will be used for determination of certain occlusal events, and complete 3D models of the teeth will illustrate occlusion of the entire tooth form. In this way, the influence of the different geometric factors on each other, and how they interact to create a final functional tooth form, can be examined.

The objective is to create models in which: 1) occlusion between upper and lower models occurs correctly (according to geometry outlined below); 2) advantageous functional shape parameters are adhered to; 3) the overall morphology of models is as similar as possible to real teeth; and 4) the function of real teeth is emulated. This extends the work from the ideal shapes derived previously (Evans and Sanson, 2003) to more realistic approximations of mammalian teeth.

While testing the models will increase our understanding of the function and geometry of basic tooth patterns, it will also allow us to investigate the influence of particular components, such as the protocone, on the overall form and function of the upper and lower teeth. Any differences between models and real teeth may provide information about constraints on mammalian teeth (Evans and Sanson, 2003) and factors that may limit tooth design.

A major impediment to investigations of tooth geometry has been the difficulty in examining 3D shapes and modes of occlusion, where previous models were often 2D representations of 3D models (Evans et al., 2001). The use of computer techniques for 3D representation assists the investigation of these geometrical problems. Hypotheses about tooth geometry from earlier analyses will be examined by creating 3D representations of models previously only presented in 2D.

Occlusal Geometry

Geometry of two simple blades occluding with each other will be considered first. Tooth occlusion will occur along a linear vector (the occlusal vector). The simplest case is for a blade to lie in a plane (and therefore forms a 2D curve); for two blades to align correctly, they must lie in the same plane in space (Fig. 2a), and the occlusal vector will be perpendicular to the normal of the plane (i.e., it will lie in the plane). The plane can be vertical (Fig. 2a) or at an angle to the vertical (Fig. 2b). The latter is the case for the model of carnassial teeth discussed in Mellett's (1981) study, and both were used in the single-bladed models of Evans and Sanson (2003).

An important derivation from this is the two-plane mode of occlusion (Greaves, 1972; Kay and Hiiemae, 1974; Crompton et al., 1994; Evans and Sanson, 2003). In this case, there are two blades on each model (Fig. 3a); each blade lies in a different plane, and the occlusal vector is parallel to the intersection of the two planes (Fig. 3b,c). This can be extended to show how the two-plane mode can be extended to four planes to allow two phases of occlusion (fig. 3 in Fortelius, 1985). The occlusal vector of teeth working in the two-plane mode of occlusion can be calculated from isolated teeth (Kay and Hiiemae, 1974).

The more general case is that the shape of the 2D projection along the occlusal vector is the same for

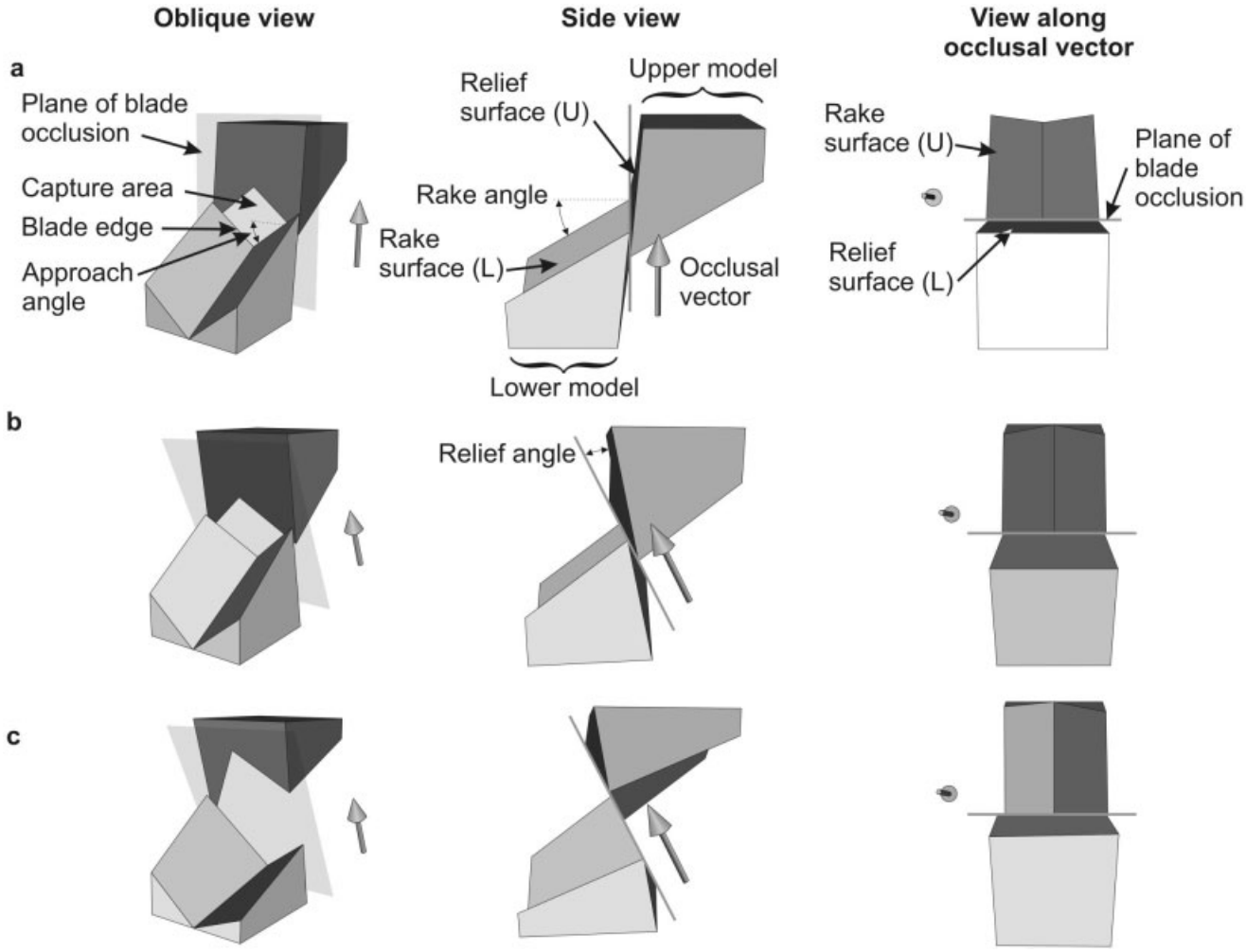

Fig. 2. Simple single-bladed models used as starting points for modeling mammalian teeth, illustrating occlusal geometrical principles: (**a**) symmetrical with vertical movement; (**b**) symmetrical with latero-vertical movement; (**c**) asymmetrical with latero-vertical movement. The blade edge and rake and relief surfaces of the upper (U) and lower (L) models are indicated. The lower model moves according to the occlusal vector (solid arrow), and occluding blade edges always lie in the plane of blade occlusion (transparent gray plane). In all figures, upper model is dark, lower is light. Additional terms defined in text. Light source for all 3D models comes directly from the viewer (like a headlight), so the more perpendicular to the viewer, the lighter the shading.

two occluding blades or teeth. This includes multiple planes, curves, and a combination of the two with planes separated by curved joins (Fig. 4).

MATERIALS AND METHODS

Models of several mammalian tooth forms were constructed according to the following procedure. For each tooth form, the surfaces of cusps and crests (and basins when present) were modeled as polygons in 3D space where the vertices of each polygon were designated by x, y, z coordinates. The lower model moves with respect to the upper model according to the "occlusal vector," the direction of lower tooth movement. Occluding crests were constructed according to the geometry described above to ensure proper alignment in all models. The tooth structures were represented in Virtual Reality Modeling Language (VRML; Evans et al., 2001; Evans and Sanson, 2003), which allows animation of 3D structures to demonstrate occlusion.

The models of single- and double-bladed tools constructed in the study by Evans and Sanson (2003) were used as starting points, and these are shown in Figures 2 and 3. These simple shapes are excellent initial shapes for modeling teeth because they have been explicitly derived: their shape and the reasoning behind their construction are precisely known. In Evans and Sanson (2003), the simple shapes were made by starting with regular geometrical shapes (cube and triangular prism) and incorporating functional criteria without reference to real tooth forms. There are many similarities between the simple shapes and real tooth structures before additional modifications are made, but the objective of this study is to make models that specifically emulate mammalian teeth.

The simple models may represent entire mammalian teeth, or components of the teeth, so that each model tooth is constructed from one or more duplicates of the starting models. Successive changes were made to the models in a step-by-step process in order to more closely emulate real tooth forms. For instance, relative positions of crests and cusps and the angles of certain surfaces may be changed in the model so they more accurately represent the shape of the real tooth. However, no major changes were made to features such as the number of blades, so a reasonable degree of similarity is still apparent between the final models

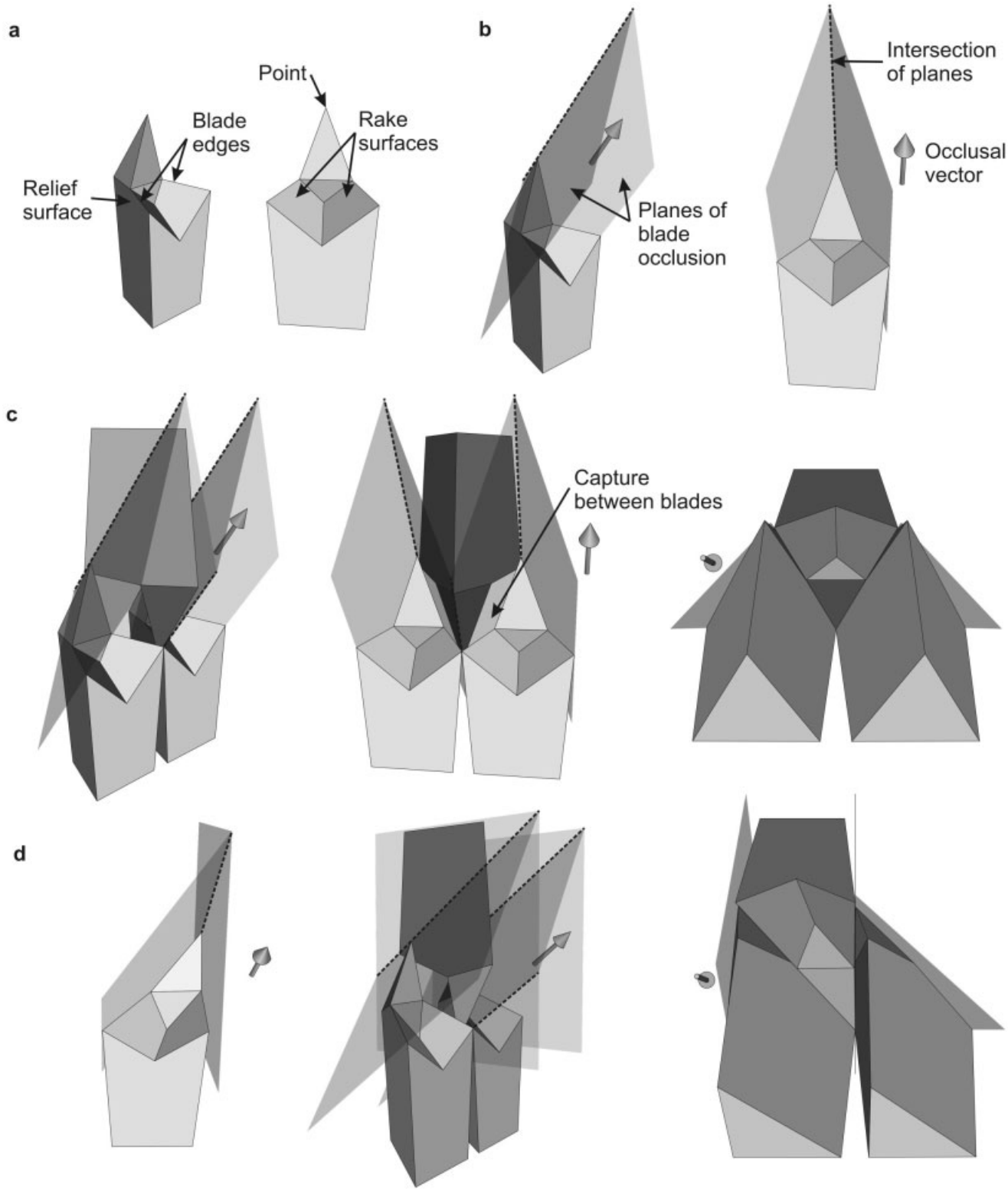

Fig. 3. Simple double-bladed models used as starting points for modeling mammalian teeth, illustrating occlusal geometrical principles: (**a**) protoconoid with latero-vertical movement; (**b**) showing planes of blade occlusion; (**c**) two lower and one upper protoconoid in occlusion; (**d**) right-angled protoconoid. The intersection of planes of blade occlusion is indicated by a dashed line, which is parallel to the occlusal vector. Other conventions follow Figure 2.

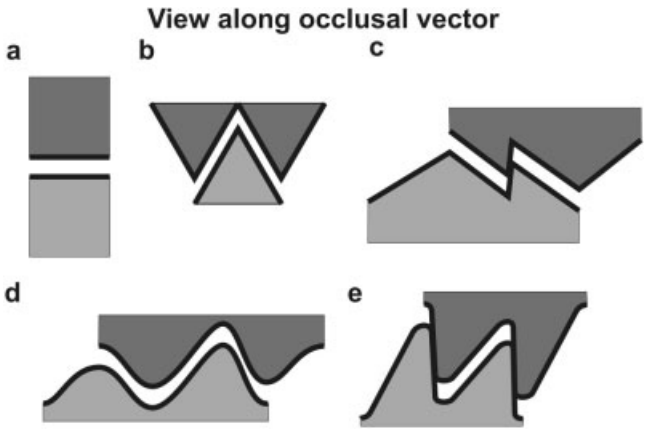

Fig. 4. Crest shapes that are possible for occluding upper (dark) and lower (light) teeth with blades (thick lines) when the lower moves along a linear occlusal vector. The shapes are viewed along the occlusal vector and are separated vertically on the page a small amount for clarity. **a:** Single-bladed model. **b:** Double-bladed model. **c:** Planes in various orientations. **d:** Curves. **e:** Straight lines joined by curves where the cusps are located.

and the starting shapes. All changes were documented to make clear the modifications to these shapes that were necessary.

The initial shapes and final tooth models all conform to eight functional parameters that have been considered a priori to be important in the function of tools for dividing tough foods. High toughness is the main reason for requiring bladed teeth (Lucas, 1979; Lucas and Luke, 1984) and these tooth forms appear to be most adapted to fracturing tough foods (Evans and Sanson, 2003, in press). The functional parameters are defensible in terms of machine tool engineering and dental function. These were described in detail previously (Evans and Sanson, 2003) and are: tip and cusp sharpness for points; edge sharpness, rake, relief, and approach angles; food capture and fragment clearance for blades. As an example of how these characteristics can be directly related to the force and energy to fracture food, the rake angle is the angle of the leading blade face to a line perpendicular to the occlusal vector (Fig. 2a). An increase in the rake angle (decreasing the included angle of the blade) results in less force and energy being needed to divide food. Brief definitions for some of the other functional parameters are as follows: the relief angle is the angle between the relief surface and the occlusal vector (Fig. 2b); the approach angle is the angle between the long axis of a blade and a line perpendicular to the occlusal vector (Fig. 2a); and capture area is the area enclosed by a concave blade that traps food (Fig. 2a).

Tooth Forms to Be Modeled

As the models were designed to emulate the shape, movement, and function of mammalian teeth, specimens from museum collections of several examples of the general tooth forms were examined to find broad characteristics of each form. The general shape of upper and lower tooth components and manner of occlusion for each tooth form are described below. In some cases additional minor cusps and cingula (small enamel ledges or rims that surround part of the tooth) are also present, which often vary greatly between species, but to simplify the modeling process these are not considered here. The object is to model the generic characteristics of the tooth forms.

Carnassials. Molars or premolars with a single long crest with a large, symmetrical V-shaped notch (Fig. 5a–d), often with a more pronounced central notch (carnassial notch) which aids in dividing tough food at the end of a stroke (Van Valen, 1969; Abler, 1992). The upper and lower crests are relatively similar in shape (Butler, 1946; Van Valen, 1966; Mellett, 1981, 1985; Van Valkenburgh, 1991; Bryant and Russell, 1995). They occur in carnivorans (Carnivora), fossil creodonts (Hyaenodontia), and marsupials (e.g., Thylacoleonidae).

Insectivore premolars. The teeth have a single, long, notched crest, the ends of which are unequal in height, creating an asymmetrical notch. They may occlude with the crests of other premolars or of molars, and are partially molariform (Butler, 1937, 1939; Mills, 1966; Slaughter, 1970; Freeman, 1981). The premolars modeled here are more akin to upper premolars that occlude with the first lower molar. They are found in insectivorans and microchiropterans.

Zalambdodont molars. The teeth comprise a single, large cusp with two crests leading from it, forming a V-shaped "ectoloph" viewed from above (Fig. 5e–h). One crest of the ectoloph is often approximately transverse to the tooth row, and the crests of the upper and lower molars are generally similar (Butler, 1937, 1941; McDowell, 1958; Mills, 1966). This tooth form is found in solenodons (Solenodontidae), tenrecs (Tenrecidae), and golden moles (Chrysochloridae). There is a basic topographic similarity to symmetrodonts (e.g., *Kuehnotherium*), pantotheres (e.g., *Amphitherium, Peramus*), *Zalambdalestes, Palaeoryctes,* and the marsupials *Necrolestes* and *Notoryctes* (Carroll, 1988).

Dilambdodont molars. The V-shaped ectoloph of the zalambdodont has been essentially duplicated in each of the upper and lower molars (Butler, 1941; Mills, 1966). On the upper molar, the crests leading from these two large cusps form a W-shaped ectoloph, where all of the crests reach the buccal edge of the tooth (Fig. 5k,l). A third major cusp is positioned laterally, dorsally, and anteriorly on the upper tooth (large cusp at the top of Fig. 5l), and is often associated with one or two additional smaller cusps. On the lower tooth, the posterior cusp is lower than the anterior one and forms a basin which occludes with the upper lateral cusp (Fig. 5i,j). During occlusion, the leading face of the lower posterior cusp meets the leading face of the upper lateral cusp (Mills, 1966; Kallen and Gans, 1972). These are found in shrews (Soricidae), moles (Talpidae), tree shrews (Tupaiidae), microbats (Microchiroptera), and extinct groups such as nyctitheriids (Carroll, 1988), *Palaeotherium*, brontotheres, chalicotheres (Perissodactyla), *Anoplotherium* (Artiodactyla), and *Pantolambda* (Pantodonta) (Butler, 1982).

Tribosphenic molars. The tribosphenic form is similar to the dilambdodont form in having three main cusps on the upper tooth and two on the lower (Fig. 5m–p). The main difference from the dilambdodont form is that the ectoloph is not as strongly W-shaped—the two center crests of the ectoloph (collectively called the centrocrista) do not reach the buccal edge of the tooth (Butler, 1982; Mills, 1966; Crompton and Hiiemae, 1970). The tooth form modeled here can also be considered dilambdodont (Butler, 1941, 1996) or predilambdodont (Johanson, 1996; Wroe et al., 2000). These are found in primitive mammals such as *Aegialodon, Pappotherium, Didelphodus* (Carroll, 1988), marsupials (Didelphidae), and in a reversed form in the pseudotribosphenic molars of *Shuotherium*, where the basin in the lower tooth is anterior instead of posterior (Chow and Rich, 1982).

Models

Carnassials. The model of the carnassial was based on the symmetrical single-bladed tool with a single long blade with a V-shaped notch and a latero-vertical occlusal vector (Fig. 2b). In order to approach more closely the carnassial tooth shape, the rake angle of the model was increased and a "carnassial notch" was added. It allows a greater concentration of forces due to the increased approach angle and due to the reduced amount of material between the teeth once the central notches come into contact.

Insectivore premolars. The asymmetrical single-bladed model was used as the basis for the premolars of some insectivores (Fig. 2c). The rake angle was increased and the size of the smaller cusp decreased.

Zalambdodont molars. The starting point for the zalambdodont molar model was the basic protoconoid structure, which is

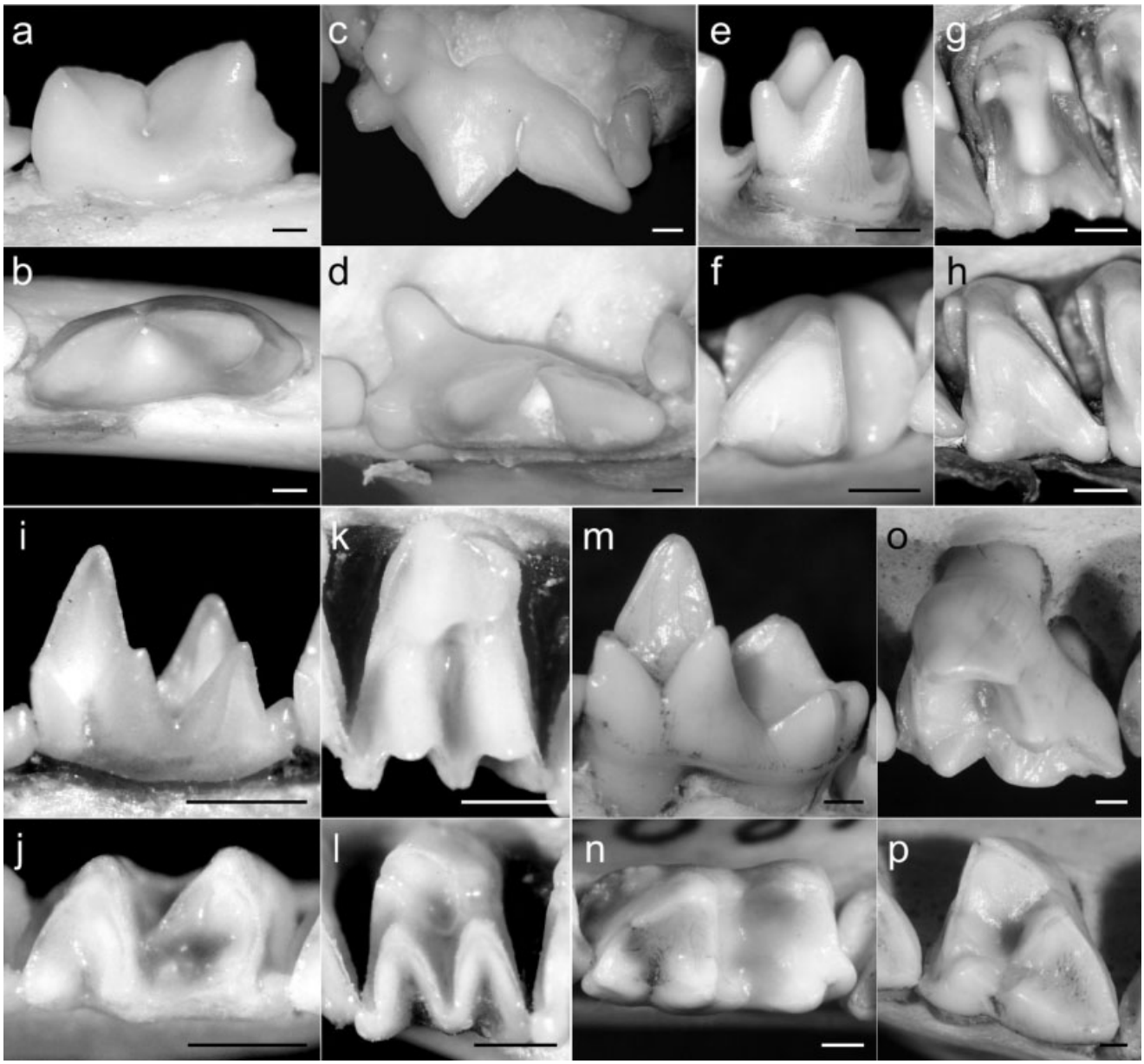

Fig. 5. Mammalian tooth forms modeled in this study. **a–d:** Carnassial, PM^4 (**a,b**) and M_1 (**c,d**) (*Felis catus*; Carnivora: Felidae). **e–h:** Zalambdodont, M^2 (**e,f**) and M_2 (**g,h**) (*Tenrec ecaudatus*; Insectivora: Tenrecidae). **i–l:** Dilambdodont, M^2 (**i,j**) and M_2 (**k,l**) (*Myotis daubentoni*; Chiroptera: Vespertilionidae). **m–p:** Tribosphenic, M^2 (**m,n**) and M_2 (**o,p**) (*Didelphis virginiana*; Didelphimorphia: Didelphidae). Lower right-side teeth in lingual (**a,e,i,m**) and occlusal (**b,f,j,n**) views; upper right-side teeth in lingual (**c,g,k,o**) and occlusal (**d,h,l,p**) views. Anterior to left. Scale bars = 1 mm.

a fundamental cusp-crest structure found in many tooth forms (Evans and Sanson, 2003). The base of the protoconoid is an equilateral triangle, and two of the top edges form blades, each of which has a V-shaped notch (Fig. 3). There are three main points on the protoconoid, which occur at the end of blades, and the point at the junction of the two blades is the tallest point on the model. The lower model moves with a latero-vertical occlusal vector. The upper and lower zalambdodont molars were modeled as "right-angled" protoconoids, where the base of the protoconoid is a right-angled triangle with one blade perpendicular to the side of the model and the other oblique (Fig. 3d).

Dilambdodont molars. Each of the upper and lower dilambdodont molars was modeled as two "right-angled" protoconoids in series. A third protoconoid was added on the lateral side of the upper model, and "*en echelon* shear" occurs, where a blade from the lower model sequentially occludes with two or more blades of the upper (Crompton and Sita-Lumsden, 1970), between the lower model and two protoconoids in the upper model.

Tribosphenic molars. The tribosphenic molar model was based on the basic dilambdodont model, the main difference being that the center cusp of the ectoloph does not reach the buccal edge. In addition, the crests of the centrocrista are not concave in the same manner as the dilambdodont form (Butler, 1996).

Improved dilambdodont molars model. To illustrate how some of the differences between the models and real teeth influence the form of the models, a second model of the dil-

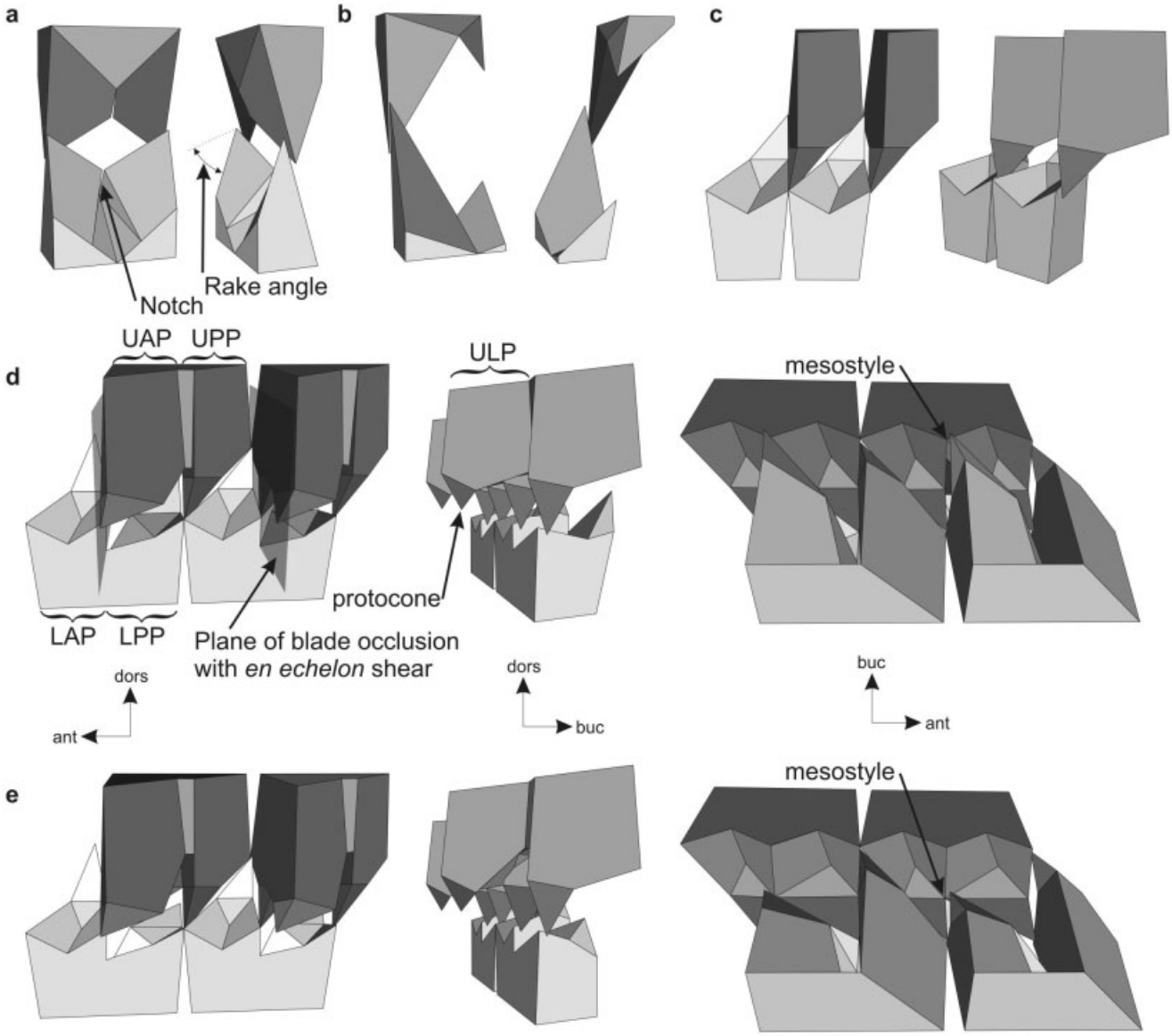

Fig. 6. Modified models of mammalian tooth forms: (**a**) carnassial; (**b**) insectivore premolar; (**c**) zalambdodont; (**d**) dilambdodont; (**e**) tribosphenic. A single upper and lower model is shown for carnassial and insectivore premolar; two upper and two lower models are shown for zalambdodont, dilambdodont and tribosphenic. Planes of blade occlusion are shown in **d** to illustrate *en echelon* shear. The main difference in the dilambdodont and tribosphenic models is the distance of the mesostyle from the buccal edge of the model. ant, anterior; buc, buccal; dors, dorsal. LAP, lower anterior protoconoid; LPP, lower posterior protoconoid; UAP, upper anterior protoconoid; ULP, upper lateral protoconoid; UPP, upper posterior protoconoid. Light source from viewer.

ambdodont form was constructed. This model incorporates an anterior component to the dorsolingual occlusal vector, as is the case for in vivo teeth; the transverse crest of the protoconoids is no longer directly perpendicular to the edge of the tooth; the paracone is smaller than the metacone, with a consequently smaller talonid basin and shorter hypoconid; additional cusp occlusion relief is added behind some points; and the upper ectoloph crests and preprotocrista are crescentic.

Crompton and Sita-Lumsden (1970) model. The illustrations in the study of Crompton and Sita-Lumsden (1970) (redrawn in Fig. 1) were used to generate a 3D reconstruction of their model. A 3D shape was chosen that matched all illustrations from different views as closely as possible.

RESULTS

The models of all tooth forms are shown in Figure 6. The conventional dental nomenclature of these forms will be used to describe the models (Crompton, 1971; Kay and Hiiemae, 1974), and is illustrated in Figure 7a. The carnassial (Fig. 6a) has a larger rake angle, making the tooth narrower, and a very sharp notch at the center of the blade. The insectivore premolar has a single blade with a very tall cusp and a shorter cusp connected by a crest that allows cap-

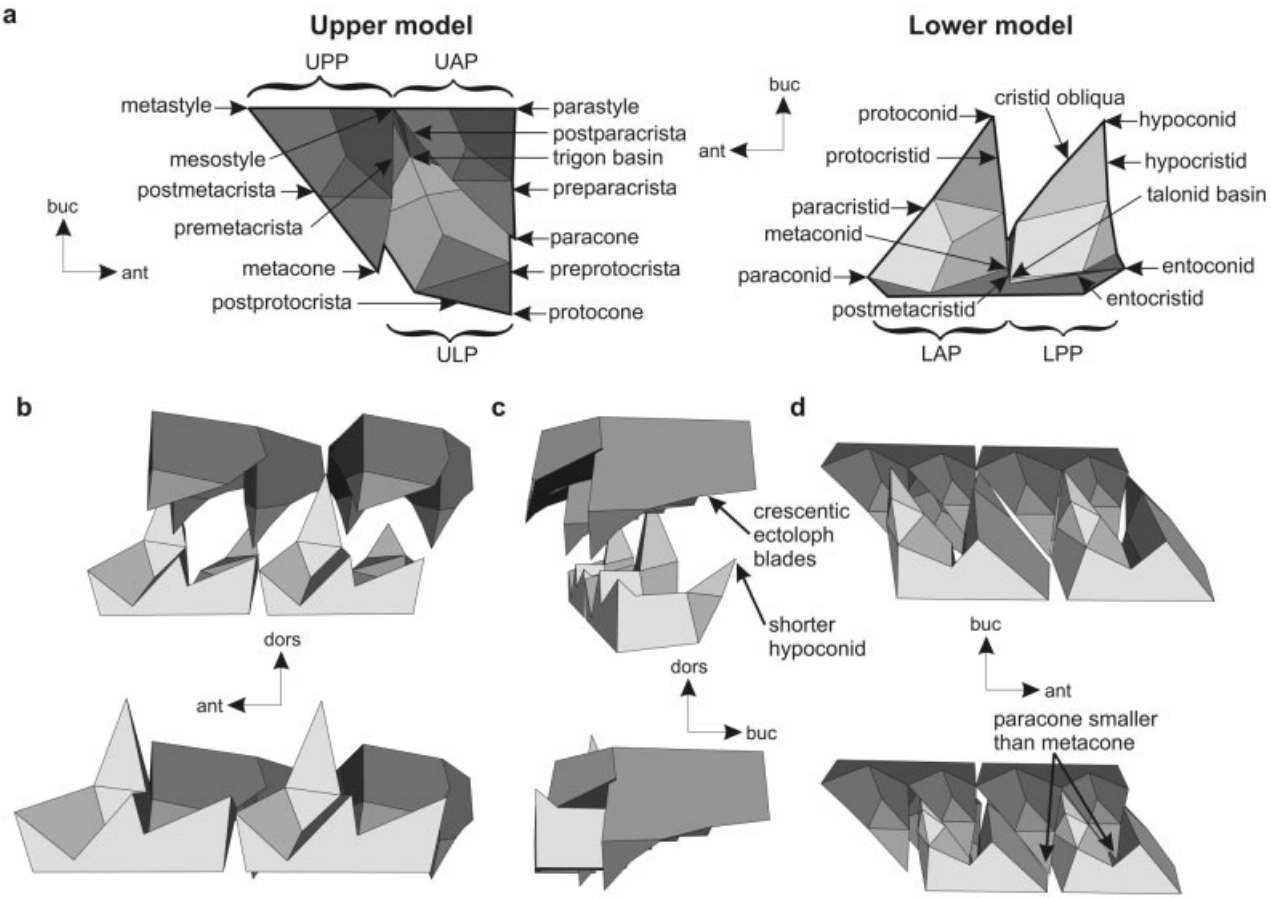

Fig. 7. Improved model of dilambdodont molars incorporating an anterior component to the previously dorsolingual movement, crescentic crests on the upper ectoloph crests and preprotocrista, and paracone smaller than the metacone, with consequently smaller talonid basin and shorter hypoconid. **a:** Nomenclature of upper and lower dilambdodont molars, and separate views of the upper and lower dilambdodont models. The centrocrista comprises the postparacrista and the premetacrista. Lingual (**b**), posterior (**c**), and buccal-occlusal (**d**) views of two upper and two lower model molars just after occlusion has started (top) and at centric occlusion (bottom), where the lower molar is at its dorsal maximum and the protocone is at the base of the talonid basin. Abbreviations and conventions follow Figure 6.

ture (Fig. 6b). In the two upper and two lower zalambdodont molars shown in Figure 6c, each zalambdodont molar occludes with two opposing models.

As well as the two protoconoids in serial arrangement, the model of the upper dilambdodont tooth has a third protoconoid (with the protocone as the main cusp) in a lateral position (Fig. 6d). Two main functional changes result: on each tooth, two additional occluding blades and a flat "crushing" basin are created. The crushing surfaces are the rake surfaces of the lower posterior and upper lateral protoconoids. These are the talonid and the trigon basins, respectively, and they meet at the end of the occlusal stroke. The posterior blade of the lower anterior protoconoid occludes with two blades in the one stroke: with the anterior blade of the upper lateral protoconoid and the anterior blade of the upper lateral protoconoid. This *en echelon* shear is shown in Figure 6d, where the plane of blade occlusion passes through the blades that occlude. Another blade is added to the lateral edge of the lower posterior protoconoid (the previously non-occluding third edge) that occludes with the posterior blade of the upper lateral protoconoid.

The main modifications in creating the dilambdodont model result from the addition of protocone. These can be summarized as follows:

1. The lower posterior protoconoid main cusp (hypoconid) was reduced in height and/or moved buccally to prevent it from colliding with the rake surface of the upper lateral protoconoid.
2. Two crests were added to the lower models against which the crests of the upper lateral protoconoid main cusp (protocone) occlude: the crest running from the posterior cusp of the lower anterior protoconoid (postmetacristid) and the crest on the exit structure of the lower posterior protoconoid (entocristid).

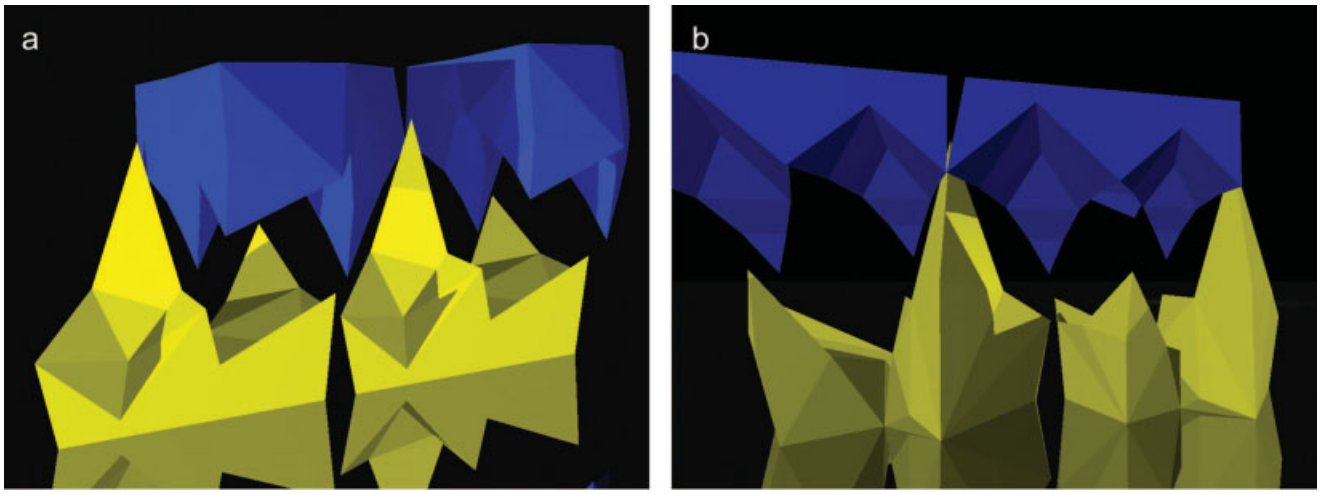

Fig. 8. Three-dimensional shaded reconstruction of the improved dilambdodont model. **a:** Lingual view, anterior to left. **b:** Buccal view, anterior to right. Multiple light sources.

3. The height of the anterior crest of the lower posterior protoconoid (cristid obliqua) was reduced so that it no longer connected to the posterior cusp of the lower anterior protoconoid (metaconid) and instead terminated near the base of the lower anterior protoconoid main cusp (protoconid). This allowed the anterior crest of the upper lateral protoconoid (preprotocrista) to shear against the posterior crests of the lower anterior protoconoid (protocristid and postmetacristid).
4. The basin of the lower posterior protoconoid (talonid basin) was deepened to form relief behind the new crests (postmetacristid and entocristid).

The main modification made in order to construct the tribosphenic model was the movement of the mesostyle from the buccal edge of the tooth, requiring lingual and dorsal movement of the hypoconid (Fig. 6e). The shape of the main cusps in the upper molars is now further removed from the initial protoconoid shape.

Additional changes were made for the improved dilambdodont model to increase the similarity to real dilambdodont teeth (Figs. 7, 8). Three different views of the 3D reconstruction of Crompton and Sita-Lumsden's (1970) model are shown in Figure 9. The blades of the reconstructed model fit within planes and are therefore 2D curves.

The supplementary material contains VRML files for all model teeth constructed here, showing the 3D shape and animated occlusion of the models, and is also available from the first author.

DISCUSSION

The models constructed above have significant similarities to the tooth forms on which they were

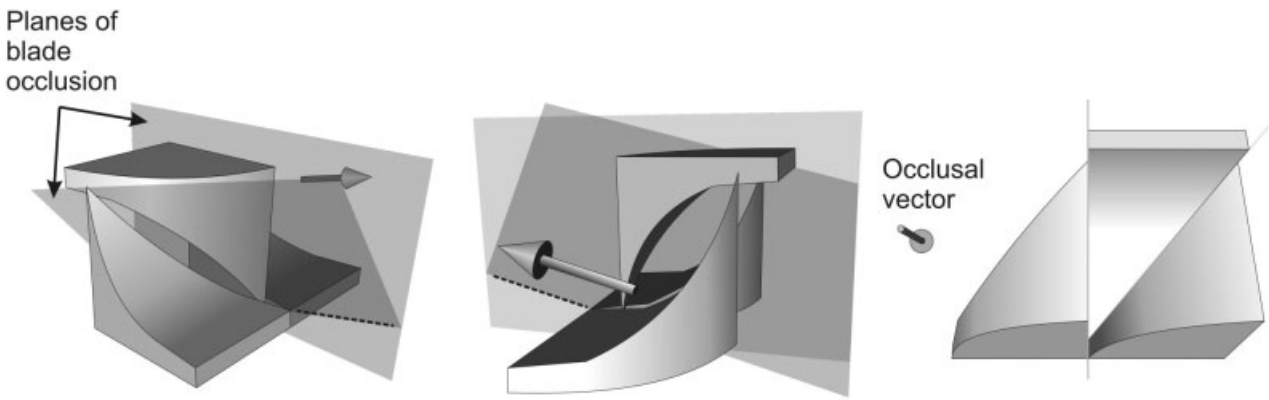

Fig. 9. Three-dimensional reconstruction of model shown in Crompton and Sita-Lumsden (1970), showing that both of the blades on the model are two-dimensional curves, as each lies in a plane. Light source from viewer.

modeled, and it is argued that they would function in the same manner as the original teeth due to the requirements of the geometries of occlusion and function being satisfied. The similarities are now substantially more extensive than the approximate ones of the starting models.

Comparisons of Models and Real Teeth

The models very closely mimic the shape and occlusion of mammalian tooth forms. However, there are a number of notable differences between each model and its corresponding tooth form. Some of these point to factors that constrain shape in mammalian teeth that are not considered in the models, but others reveal additional complexity in the function of mammalian dentitions.

Robustness. Compared to the idealized perfect points of the model, the cusp tips of teeth are thicker and the embrasures into which they fit are wider. This is particularly true for the zalambdodont, dilambdodont, and tribosphenic forms, where the cusp tips are often rounded in the anteroposterior direction. This is most probably related to the requirement of increased strength at the tip of the cusps, where thicker teeth will be able to withstand greater stresses. The occluding embrasures must then be wider to accommodate the fatter cusps. Development may also constrain the tooth shapes, limiting the maximum pointedness of cusps that can be produced in ontogeny. Real teeth are often broader and rounder at the base of the cusps compared to the models, again probably related to increased strength and support.

Although the cusps and crests of dilambdodont and tribosphenic teeth do not have as high tip, cusp, and edge sharpnesses as the models, they do represent an ingenious solution that maintains relatively high tip and edge sharpnesses while ensuring that proper occlusion occurs between crests and allowing additional reinforcement of the cusp. The pointed cusps of the models (Fig. 6d,e) would probably produce dangerously high stress concentrations that may fracture the cusp; however, rounding the entire cusp tip to strengthen it will reduce tip and edge sharpnesses. Instead, the cusp tips are rounded in the anteroposterior direction, while being relatively flat on the buccal face. Such cusps have high tip and edge sharpness compared to a rounded cusp but allow occlusion between crests and would resist fracture to a greater extent.

Cusp occlusion relief. In dilambdodont and tribosphenic molars, there is often significant relief behind the points on one tooth where another cusp occludes with it, which is termed cusp occlusion relief (described in further detail in Evans, 2003, in press; this differs from occlusal relief discussed in Fortelius and Solounias, 2000). This is very similar to the relief angle shown in Figure 2b, except that the relief is behind a cusp rather than a crest. Relief is found behind occlusion points of cusps such as the protoconid (relief behind the parastyle/metastyle), hypoconid (mesostyle), protocone (postmetacristid/entocristid junction lingual to the talonid basin), and to some extent the metacone (posterior cingulum on lower molar) and paracone (at the most anterior point of the cristid obliqua). Only a small amount of cusp occlusion relief occurs in the models, usually due to the creation of relief behind the crests.

Sizes of paracone and metacone. The upper models of dilambdodont and tribosphenic molars were constructed with the paracone and metacone the same size. In tribosphenic and more particularly dilambdodont teeth, the paracone is often smaller than the metacone, with the paracone closer to the buccal edge of the tooth and shorter in height. The size of the paracone affects the geometric relations between the upper and lower molars, particularly the width of the talonid basin.

When the hypoconid is lowered to accommodate the protocone in the dilambdodont model, it must also be repositioned laterally so that it still occludes with the mesostyle (due to the lateral movement of the teeth). If the metacone and paracone are the same size, the hypoconid must be shifted a large distance laterally if the height is greatly decreased, resulting in a talonid basin that is substantially wider than the anterior (trigonid) basin. In the dilambdodont and tribosphenic models, the height of the hypoconid has not been substantially reduced. Repositioning the paracone closer to the buccal edge of the tooth, in effect reducing the size of the paracone, reduces the distance from the mesostyle to the paracone, so that the hypoconid does not need to be shifted as far laterally to allow occlusion.

Shape of capture structure. The blades of the models constructed above have notched, i.e., V-shaped, capture structures. The few models of cusps or teeth that have been made previously have often implicitly or explicitly modeled the capture structure as a curved, "crescentic," or U-shaped edge (e.g., Fig. 1; Crompton and Sita-Lumsden, 1970; Mellett, 1981; Stern et al., 1989; Crompton et al., 1994; Lucas and Teaford, 1994). It seems to have been assumed that a curved edge must function better because it occurs in nature. However, a V-shaped capture structure would be more efficient than a U-shaped one, as it would concentrate forces to a greater extent, particularly at the end of the stroke. The areas of the approaching edges at the end of a stroke are smaller in an acute notch than in the case of a U-shaped capture mechanism, so the notch attains higher stress at the end of the stroke and offers a greater potential to fracture the food item. A notch will also have a higher approach angle at the end of the stroke.

The concavity in carnassial teeth is pointed (and further emphasized as the carnassial notch), as is the case for many crests in lower dilambdodont and

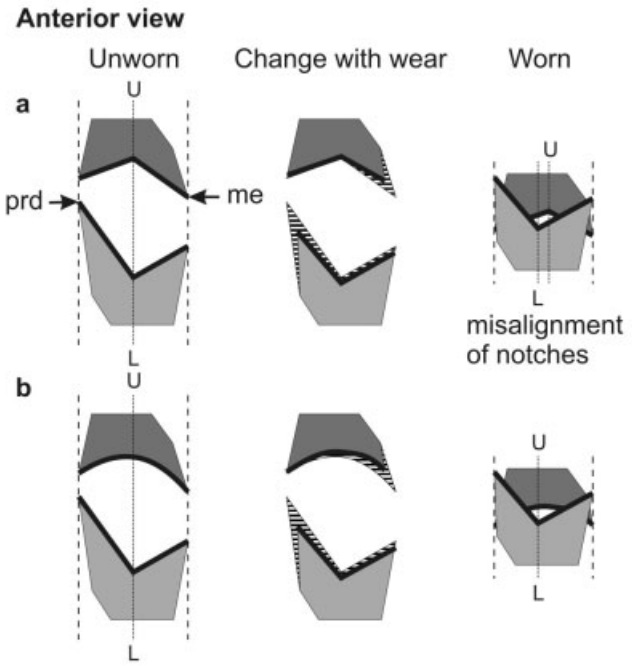

Fig. 10. The effect of wear and crest shape on the alignment of occluding notches. Each sequence (**a,b**) illustrates a particular arrangement of crests (thick lines) and notches on upper (dark) and lower (light) teeth in the unworn and worn states, and shows the change in shape after the removal of dental material by wear (horizontal hatching). **a:** Both the upper and lower crests are notched. Following wear, which mostly occurs on the end of the crest with the higher cusp (metacone (me) for the upper and protoconid (prd) for the lower), the notches no longer align in occlusion. However, when one of the crests is curved (**b**), the effects on the alignment of the notch are not as severe. Dashed lines show points at which the ends of crests occlude, dotted lines show the location of the upper (U) and lower (L) notches. Anterior view, with occlusal vector vertical.

tribosphenic teeth (e.g., microbats *Rhinolophus blasii* and *Plecotus townsendii*; marsupial *Didelphis marsupialis*). However, upper dilambdodont and tribosphenic teeth usually do not have notched ectoloph crests. This may be because a pointed notch may increase stress concentrations in the tooth at the tip of the notch, with a subsequent rise in the risk of the tooth fracturing at that point. An alternative is that it is related to the depth of tooth underneath the ectoloph crests, such that a deep, V-shaped notch would not fit.

Effects of wear on occlusion. An important difference between real teeth and the models is that the former must accommodate wear. This becomes important when we consider how tooth shape and occlusion may be affected by wear. The function of notched crests will be optimal when the notches of opposing crests align in occlusion (Fig. 10a). If notches do not align, such as when their relative positions along the crests alter after wear, there may be regions in which the approach angles of opposing crests are close to parallel, thereby reducing the effectiveness of point cutting (point cutting occurs when the long axes of two occluding blades are not parallel, so that only one point meets at a time rather than the entire length; Evans and Sanson, 2003). This will greatly decrease the effectiveness of these crests at the end of the cutting stroke. A compromise would be to maximize efficiency in one occluding crest by making it notched, and minimize potential problems of misalignment by the opposing crest being curved (Fig. 10b).

Improvements to Models

The improved dilambdodont model has now a very high level of similarity to the teeth on which it is modeled, emulating both the shape and function of these teeth (Figs. 7, 8). Additional modifications to the improved dilambdodont model could be introduced, such as movement of the lower teeth in an arc-like fashion, simulating the closing of a jaw, rather than the linear trajectory that was used. This would affect the size and orientation of the tooth components along the tooth row, depending on the distance from the condyle and its height above the tooth row, but is not likely to change the overall shape of the models to a great extent.

Influence of Protocone on Tooth Shape

The models give us the unprecedented ability to analyze the effect of the protocone on overall tooth shape. In effect, this identifies the changes that are required to create the dilambdodont and tribosphenic forms. In order to ensure proper functioning of the upper lateral protoconoid (protocone and associated crests) added to the two-protoconoid serial structure, several modifications were required. These mostly relate to the addition of crests to the lower posterior protoconoid that occlude with the newly added upper lateral protoconoid, and the shifting of the main cusp of the lower posterior protoconoid and associated crests to prevent collision with the new protoconoid.

Increasing the number of blades in close proximity (e.g., through the addition of a protocone on the upper tooth) leads to modifications in the shape and function of the adjacent blades. Capture by several of the blades (e.g., cristid obliqua, postmetacristid) is reduced or removed. This is particularly true for the centrocrista crests of the upper tribosphenic molar, where food is captured by the combination of the two crests (postparacrista and premetacrista making up the centrocrista) rather than one. The rake angles of the crests associated with both the lower posterior protoconoid (hypoconid) and the upper lateral protoconoid (protocone) are decreased, and are therefore not as efficient. Fragment clearance from the lower posterior protoconoid is impeded by the addition of a blade on the internal surface of the exit structure. This shows the influence of geometrical constraints

on the number of blades that can be added while maintaining function of all previous and newly added crests.

Autocclusion

A significant feature of teeth that must be considered is the means by which tooth components of upper and lower teeth are aligned and how their correct relationships are maintained. For instance, does the alignment of crests require additional dental or nondental structures (such as guiding cusps or ridges) that do not function in food breakdown?

Mellett (1985) introduced the term "autocclusal" to refer to occlusal alignment that is controlled by morphology rather than neurological processes. It was first applied in reference to the use of canines to aid in the alignment of the postcanine teeth, but we can extend this to include features that ensure proper alignment of teeth on the same tooth and other teeth in the tooth row. Some features of the autocclusal mechanism are obvious, such as the spacing of cusps in a tooth row to align with the corresponding embrasures in the opposing row, which can act in the same manner as the canines directing the movement of the lower jaw to ensure alignment of molars. Of greater interest is the maintenance of correct spatial relationships between other tooth features such as relief surfaces.

A simple consideration of blade occlusion may lead one to the conclusion that in order for blades to align there must be substantial contact between the relief (trailing) surfaces of two occluding crests, which would be indicative of no relief behind crests. Most previous models of teeth crests have displayed a lack of relief (Crompton and Sita-Lumsden, 1970; Stern et al., 1989; Crompton et al., 1994; Lucas and Teaford, 1994). For instance, it appears that Crompton et al. (1994) assume contact of the flat opposing relief surfaces, and therefore the absence of relief, is required for alignment of triangular cusps. However, crest relief is present in a large number of tooth forms (Evans, 2003, in press; unpubl. data). Contrary to the models, contact between flat relief surfaces is not necessary to ensure proper occlusion. The models constructed here, and their underlying geometry, show that once proper occlusion has commenced (i.e., where the tallest protoconoid in the lower zalambdodont, dilambdodont, and tribosphenic models has entered the embrasure between the two upper models, or the blades of the carnassial or premolars are in contact), autocclusal mechanisms will operate and mean that proper occlusion will follow, given a vertical or latero-vertical force applied to the lower teeth. Only the crest edges will contact (and possibly a small amount of relief surface, particularly in worn teeth), and the direction of tooth movement will be dictated by the arrangement of the crests. Therefore, relief is maintained in these teeth purely through the geometry of the tooth surface. This is the case for Mellett's (1981) model of carnassial function, where the arrangement of the blades automatically generates relief behind the blades.

Neurological requirements for alignment are therefore limited to the first (or possibly first few) contacts between upper and lower teeth (such as the protoconids of one or more molars entering the embrasure between upper molars, or contact between canines). After this first contact, the alignment of crests dictates the movement of teeth. If a vertical force were applied by the masticatory musculature, the lower jaw would be directed laterally due to the arrangement of the blades, and contact between opposing blades would be maintained. A lateral component to the occluding vector could be introduced, but it cannot be any greater than that which would cause the blades to lose contact. In essence, this shows that these tooth forms are auto-aligning, and no additional morphological guides are necessary for correct alignment in these tooth forms.

The positive rake angles of most crests will also aid the alignment of teeth (Evans and Sanson, 2003). The rake surface of a crest will tend to be pushed perpendicular to the surface by food that contacts it, and so a positive rake will push a crest towards its opposing crests. In contrast, two occluding crests with negative rake will tend to be pushed apart by the food between them.

Therian Molar Modeling

A fully explicit model of a tribosphenic-like tooth is very effective in many respects, as demonstrated above. However, very few attempts at modeling a tribosphenic-type tooth have been reported in the literature, presumably due to the perceived complexity of the tooth structure and occlusion. In reality, this can be successfully analyzed and the structure can be modeled without great difficulty, especially when approached as a modular design. A major impediment to previous work has been the difficulty in representing the dynamics of these structures using drawings alone, so this work has been aided by the use of computer reconstruction.

It seems that the only detailed attempt at modeling components of primitive therian or tribosphenic teeth is that of Crompton and Sita-Lumsden (1970). Their model of reversed triangles is similar to the blade arrangement of a right-angled protoconoid, with an oblique blade (diagonal shearing edge, dse; Fig. 1b) and perpendicular blade (transverse shearing edge, tse), each of which trap food between the opposing blades. They hypothesized that in order for both blades to maintain contact throughout a latero-vertical cutting stroke, the oblique blade must be a 3D curve. In fact, as previously explained, the main requirement is that occluding blades are the same shape (either linear or curvilinear) when viewed along the linear occlusal vector (Fig. 4). The simplest

case is for the 2D projection of a blade to be linear, in which case it is a 2D curve (as is the case for all of the models in this study), but it is possible for the blades to be curves in two or three dimensions. The model of Crompton and Sita-Lumsden (1970) then is a subset of the larger class of models outlined here.

Crompton and Sita-Lumsden's (1970) model is most easily interpreted as a cusp with two 2D crests, since a plane can be fitted to each crest as it occurs in 3D space (Fig. 9). This directly contradicts their conclusion on the limitations of tooth design. The conclusion regarding the shape of the dse comes from a mistaken belief that "the intersection of a vertical convex surface and a concave surface" must be a 3D curve (Crompton and Sita-Lumsden, 1970: 197), which, as shown by the reconstruction, is not necessarily the case.

The study of Crompton et al. (1994) considers the occlusion of tribosphenic-type molars in terms of a triangular wedge sliding in a matching "V"-shaped slot. However, it does not relate this to the model of Crompton and Sita-Lumsden (1970), nor does it explain that the triangular wedge model contradicts the hypothesis of the earlier model. This wedge model is a way of representing the two-plane mode of occlusion described above but does not explain other features of occlusion nor the function of the teeth in the manner of the functional parameters used here.

Despite the large number of possible shapes that occluding crests can adopt, they are in fact fairly restricted. In carnassials and insectivore premolars, they are largely 2D curves, and so lie in a plane. The crests of zalambdodont, dilambdodont, and tribosphenic molars are most often 2D for the majority of the crest, so that the notch of the crest lies within the plane. It is only at the ends of a crest that it becomes a 3D curve—the rounded cusp tips and embrasures mean that the crest as a whole is a 3D curve, and has the appearance of Figure 4e.

Tooth Modeling

The possible applications of geometric modeling of teeth and tooth function are extremely diverse and offer great potential for understanding the interactions of tooth shape and function. Model teeth can be used to test other hypotheses relating to possible tooth geometries and examining correlated change in structure. For instance, dental models could disentangle which differences in tooth form between species are due to factors that have a major effect on tooth function and which are merely due to correlated geometry of upper and lower teeth; for example, the extent of anterior displacement of the protocone and the angle of the postmetacrista, which are variable among dilambdodont and tribosphenic tooth forms.

The greatest potential for tooth modeling may lie in examining hypotheses of dental occlusion in fossils. Probable 3D dental morphologies can be reconstructed to a much higher level of complexity and accuracy than previously in cases where occluding teeth are unknown in the fossil record (e.g., *Shuotherium*; Chow and Rich, 1982). In evolutionary studies, it can allow the construction of a functional series of teeth (e.g., early evolution of therian molars) showing how function is maintained during the evolutionary modification of tooth forms. This may indicate limitations on changes that can be made while tooth function is maintained, and consequent endpoints in the evolution of functional morphologies. The function of extinct, and even hypothetical, tooth forms can be examined and compared to extant teeth in which the function is more extensively understood. This can aid in dietary reconstruction of fossil forms, including those with no modern analog.

Very importantly, computer modeling of complex morphological structures allows the morphologist to extend any analysis beyond the page into the full four dimensions of teeth. This allows a significant improvement over the "occlusal diagrams" that have been used for over 100 years in an attempt to illustrate the occlusion between crests and cusps of opposing teeth. Dental models will be of great use in explaining the occlusion of teeth, helping both the teacher to illustrate, and the student to observe, the true occlusion of mammalian teeth.

CONCLUSIONS

The present models incorporate many more functional characteristics than previous models (such as rake and relief of blades) and their proper occlusion is demonstrated through computer reconstructions of their spatial relations. It is encouraging, then, that the final model shapes emulate mammalian tooth shapes much more closely than any previous models. Despite the highly complex 3D shapes of carnivore and insectivore molariform teeth, the crests on them can be modeled as 2D blades. We can we can find, then, simplicity in the complexity of these tooth forms that was not previously apparent. This shows that a consideration of the geometries of both occlusion and function can allow the examination of the multifarious elements that influence tooth shape, leading to a more sophisticated analysis of the complex morphologies of the mammalian dentition.

ACKNOWLEDGMENTS

We thank John Rensberger, Betsy Dumont, Mikael Fortelius, Jukka Jernvall, Gudrun Evans, and two anonymous referees for helpful comments to improve the manuscript.

LITERATURE CITED

Abler WL. 1992. The serrated teeth of tyrannosaurid dinosaurs, and biting structures in other animals. Paleobiology 18:161–183.

Bryant HN, Russell AP. 1995. Carnassial functioning in nimravid and felid sabertooths: theoretical basis and robustness of inferences. In: Thomason J, editor. Functional morphology in vertebrate paleontology. Cambridge, UK: Cambridge University Press. p 116–135.

Butler PM. 1937. Studies of the mammalian dentition. I. The teeth of *Centetes ecaudatus* and its allies. Proc Zool Soc Lond B 107:103–132.

Butler PM. 1939. Studies of the mammalian dentition. Differentiation of the post-canine dentition. Proc Zool Soc Lond B 109: 1–36.

Butler PM. 1941. A theory of the evolution of mammalian molar teeth. Am J Sci 239:421–450.

Butler PM. 1946. The evolution of carnassial dentitions in the Mammalia. Proc Zool Soc Lond B 116:198–220.

Butler PM. 1981. Dentition in function. In: Osborn JW, editor. Dental anatomy and embryology. Oxford: Blackwell Scientific Publications. p 329–356.

Butler PM. 1982. Directions of evolution in the mammalian dentition. In: Joysey KA, Friday AE, editors. Problems of phylogenetic reconstruction. London: Academic Press. p 235–244.

Butler PM. 1996. Dilambdodont molars: a functional interpretation of their evolution. Palaeovertebrata 25:205–213.

Carroll RL. 1988. Vertebrate paleontology and evolution. New York: WH Freeman.

Chow M, Rich THV. 1982. *Shuotherium dongi*, n. gen. and sp., a therian with pseudo-tribosphenic molars from the Jurassic of Sichuan, China. Aust Mammal 5:127–142.

Crompton AW. 1971. The origin of the tribosphenic molar. In: Kermack DM, Kermack KA, editors. Early mammals. London: Academic Press. p 65–87.

Crompton AW, Hiiemae K. 1970. Molar occlusion and mandibular movements during occlusion in the American opossum, *Didelphis marsupialis* L. Zool J Linn Soc 49:21–47.

Crompton AW, Sita-Lumsden A. 1970. Functional significance of the therian molar pattern. Nature 227:197–199.

Crompton AW, Wood CB, Stern DN. 1994. Differential wear of enamel: a mechanism for maintaining sharp cutting edges. In: Bels VL, Chardon M, Vandewalle P, editors. Biomechanics of feeding in vertebrates: advances in comparative and environmental physiology 18. Berlin: Springer. p 321–346.

Evans AR. 2003. Functional dental morphology of insectivorous microchiropterans: spatial modelling and functional analysis of tooth form and the influence of tooth wear and dietary properties. Ph.D. Thesis, Melbourne: Monash University.

Evans AR. Quantifying the relationship between form and function and the geometry of the wear process in bat molars. In: Akbar Z, McCracken GF, Kunz TH, editors. Functional and evolutionary ecology of bats. Proceedings of the 12th International Bat Research Conference. New York: Oxford University Press (in press).

Evans AR, Sanson GD. 2003. The tooth of perfection: functional and spatial constraints on mammalian tooth shape. Biol J Linn Soc 78:173–191.

Evans AR, Sanson GD. The biomechanical properties of insects in relation to insectivory: cuticle thickness as an indicator of insect 'hardness' and 'intractability'. Aust J Zool (in press).

Evans AR, Harper IS, Sanson GD. 2001. Confocal imaging, visualization and 3-D surface measurement of small mammalian teeth. J Microsc 204:108–118.

Fortelius M. 1985. Ungulate cheek teeth: developmental, functional, and evolutionary interrelations. Acta Zool Fennica 180: 1–76.

Fortelius M, Solounias N. 2000. Functional characterisation of ungulate molars using the abrasion-attrition wear gradient: a new method for reconstructing paleodiets. Am Mus Novit 3301: 1–36.

Freeman PW. 1981. A multivariate study of the family Molossidae (Mammalia, Chiroptera): morphology, ecology, evolution. Field Zool 7:1–173.

Greaves WS. 1972. Evolution of the merycoidodont masticatory apparatus (Mammalia, Artiodactyla). Evolution 26:659–667.

Gregory WK. 1916. Studies on the evolution of the primates. I. The Cope-Osborn 'Theory of Trituberculy' and the ancestral molar patterns of the primates. Bull Am Mus Nat Hist 35:239–355.

Jernvall J. 1995. Mammalian molar cusp patterns: developmental mechanisms of diversity. Acta Zool Fennica 198:1–61.

Johanson Z. 1996. Revision of the Late Cretaceous North American marsupial genus *Alphadon*. Palaeontog Abt A 242:127–184.

Kallen KC, Gans C. 1972. Mastication in the little brown bat, *Myotis lucifugus*. J Morphol 136:385–420.

Kay RF, Hiiemae KM. 1974. Jaw movement and tooth use in recent and fossil primates. Am J Phys Anthropol 40:227–256.

Lucas PW. 1979. The dental-dietary adaptations of mammals. N Jb Geol Paläont Mh 1979:486–512.

Lucas PW, Luke DA. 1984. Chewing it over: basic principles of food breakdown. In: Chivers DJ, Wood BA, Bilsborough A, editors. Food acquisition and processing in primates. New York: Plenum Press. p 283–301.

Lucas PW, Teaford MF. 1994. Functional morphology of colobine teeth. In: Davies AG, Oates JF, editors. Colobine monkeys: their ecology, behaviour and evolution. Cambridge, UK: Cambridge University Press. p 173–203.

McDowell SB Jr. 1958. The Greater Antillean insectivores. Bull Am Mus Nat Hist 115:113–214.

Mellett JS. 1981. Mammalian carnassial function and the 'Every Effect'. J Mammal 62:164–166.

Mellett JS. 1985. Autocclusal mechanisms in the carnivore dentition. Aust Mammal 8:233–238.

Mills JRE. 1966. The functional occlusion of the teeth of Insectivora. J Linn Soc (Zool) 46:1–25.

Osborn HF. 1888. The evolution of mammalian molars to and from the tritubercular type. Am Nat 22:1067–1079.

Osborn HF. 1897. Trituberculy: a review dedicated to the late Professor Cope. Am Nat 31:993–1016.

Slaughter BH. 1970. Evolutionary trends of chiropteran dentitions. In: Slaughter BH, Walton DW, editors. About bats: a chiropteran biology symposium. Dallas: Southern Methodist University Press. p 51–83.

Stern D, Crompton AW, Skobe Z. 1989. Enamel ultrastructure and masticatory function in molars of the American opossum, *Didelphis virginiana*. Zool J Linn Soc 95:311–334.

Van Valen L. 1966. Deltatheridia, a new order of mammals. Bull Am Mus Nat Hist 132:1–126.

Van Valen L. 1969. Evolution of dental growth and adaptation in mammalian carnivores. Evolution 23:96–117.

Van Valkenburgh B. 1991. Iterative evolution of hypercarnivory in canids (Mammalia: Carnivora): evolutionary interactions among sympatric predators. Paleobiology 17:340–362.

Wroe S, Ebach M, Ahyong S, Muizon C de, Muirhead J. 2000. Cladistic analysis of dasyuromorphian (Marsupialia) phylogeny using cranial and dental characters. J Mammal 81:1008–1024.